Climate of the Past

Open Access

Discussions

Reconstruction of the March–August PDSI since 1703 AD based on tree rings of Chinese pine (*Pinus tabulaeformis* Carr.) in the Lingkong Mountain, southeast Chinese loess Plateau

Q. Cai[1], Y. Liu[1,2], Y. Lei[1], G. Bao[3], and B. Sun[4]

[1]The state key laboratory of Loess and Quaternary Geology, Institute of Earth Environment, Chinese Academy of Sciences, Xi'an, 710075, China
[2]Department of Environmental Science and Technology, School of Human Settlements and Civil Engineering, Xi'an Jiaotong University, Xi'an, 710049, China
[3]Key Laboratory of Disaster Monitoring and Mechanism Simulating of Shaanxi Province, Baoji University of Arts and Sciences, Baoji, 721013, Shaanxi, China
[4]Department of Resources, Environment, and Urban Sciences, Xianyang Normal University, Xianyang, 712000, China

Title Page

Abstract	Introduction
Conclusions	References
Tables	Figures

|◄ | ►|

◄ | ►

Back | Close

Full Screen / Esc

Printer-friendly Version

Interactive Discussion

Reconstruction of the March–August PDSI based on tree rings of Chinese pine

Q. Cai et al.

Abstract

We utilized tree-ring cores, collected from three sites at Lingkong Mountain located in the southeast part of the Chinese Loess Plateau (CLP), to develop a regional ring-width chronology. Significant positive correlations between the tree-ring index and the monthly Palmer drought severity index (PDSI) were identified, indicating that the radial growth of trees in this region was moisture-limited. The March–August mean PDSI was quantitatively reconstructed from 1703 to 2008 with an explained variance of 46.4 %. Seven dry periods during 1719–1726, 1742–1748, 1771–1778, 1807–1818, 1832–1848, 1867–1932 and 1993–2008 and six wet periods during 1727–1741, 1751–1757, 1779–1787, 1797–1805, 1853–1864 and 1934–1957 were revealed in our reconstruction. Among them, 1867–1932 and 1934–1957 were identified as the longest dry and wet periods, respectively. On the centennial scale, the 19th century was recognized as the driest century. The drying tendency since 1960s was evident, however, recent drought was still within the frame of natural climate variability based on the 306 yr PDSI reconstruction. The warm and dry phases of Lingkong Mountain were in accordance with changes in the East Asian summer monsoon (EASM) strength, they also showed strong similarity to other tree-ring based moisture indexes in large areas in and around the CLP, indicating the moisture variability in the CLP was almost synchronous and closely related with EASM variation. Spatial correlation analysis suggested that this PDSI reconstruction could represent the moisture variations for most parts of the CLP, even larger area of northern China and east Mongolia. Multi-taper spectral analysis revealed significant cycles at the inter-annual (2.0–7.8 yr), inter-decadal (37.9 yr) and centennial (102 yr) scales, suggesting the influence of ENSO and solar activity on moisture conditions in the CLP. Results of this study are very helpful for us to improve the knowledge of past climate change in the CLP and enable us to prevent and manage future natural disasters.

1 Introduction

Various studies have demonstrated that the development of human society was closely related with changes in climate (Xu, 1998; Zhang et al., 2010, 2011; Büntgen et al., 2011). When climate change reaches an extreme level, it causes disaster. Drought is one of the most devastating natural disasters throughout the world, which also strongly influenced monsoon China. In 1999 and 2000, there was a persistent drought in north and northeast China, which caused a 20–30 % loss of agriculture productivity (Wei et al., 2004). At the end of the 1920s, an extraordinary drought affected most parts of China, and subsequent drought-induced famines and disease led to the death of 4 million residents in five provinces in northern China (Liang et al., 2006; Wang, 2006). An improved knowledge of the characteristics of climate change will enable us prevent and manage future natural disasters and promote the sustainable development of our society.

It is imperative to identify the features of climate changes in details based on long-term and continuous climatic proxies. Annually dated tree rings are preferable climatic proxies for extending the limited modern meteorological record by analyzing the relationship between tree-ring indexes and climatic factors, thereby reconstructing the climate history for centuries to millennia (Zhang et al., 2003; Yang et al., 2009; Linderholm et al., 2010; Büntgen et al., 2011; Zhu et al., 2009; Ohyama et al., 2013). Tree rings have been successfully used to investigate drought history throughout the world (Esper et al., 2007; Cook et al., 2010), including arid to semi-arid areas of China (Liang et al., 2006; Chen et al., 2011; Fang et al., 2012; Cai and Liu, 2013).

The Chinese Loess Plateau (CLP), one of the cradles of ancient Chinese civilization, covers a large region in the north of China and is one of the most intensive areas of soil and water loss in the world, partly due to limited water resources (Gao et al., 2011). Recent studies have shown that the warm-dry trend since the 1950s is clearly evident in the CLP (Yao et al., 2005; Ma and Fu, 2006) and will inevitably lead to the eco-environmental deterioration of this vast region. Investigations of the natural climate

background of the CLP are crucial for understanding the processes and characteristics of climate change in this region as well as the current status of the climate, which will contribute to policy guidance from the government. To date, few dendroclimatological studies have been conducted in the central part of the CLP (Du et al., 2007; Cai et al., 2008; Koretsune et al., 2009) because of the scarcity of old trees due to natural geographical conditions and historical reasons. However, previous studies in the marginal area of the CLP (Gao et al., 2005; Fang et al., 2012; Cai and Liu, 2013; Cai et al., 2013) have greatly contributed to our understanding of tree growth–climate relationships and climate change in this region. Even though, additional efforts are required to increase the spatial and temporal coverage, creating opportunities for a wide range of detailed local-to-regional climatological studies in this region (Linderholm et al., 2013).

This paper describes the development of a new long regional tree-ring chronology of the Chinese pine from Lingkong Mountain in the southeast CLP. The main objectives of this work were to (1) determine the response of tree-ring growth to climate; (2) use of the ring-width chronology to develop a 306 yr Palmer drought severity index (PDSI) reconstruction; (3) detect the temporal and spatial representations of this reconstruction as well as the possible driving factors.

2 Materials and methods

2.1 Study area and climate

Lingkong Mountain (112°01′–112°15′ E, 36°31′–36°43′ N) is located in the southeast region of the CLP. The altitude of Lingkong Mountain generally ranges from 1600 m a.s.l. to 1850 m a.s.l., and the highest peak is 1953 m a.s.l. At the studied sites, Chinese pine (*Pinus tabulaeformis* Carr.), generally 30 m in height and growing in mountainous brown soil, is the dominant tree species, accompanied by sparse *Quercus liaotungensis* Koidz., *Populus davidiana* Dode and *Betula platyphylla* Suk. This area has a typical temperate continental climate and is subject to the influence of the

East Asian summer monsoon (EASM). It is characterized by large precipitation variability, both annually and inter-annually. Thus, droughts and floods frequently occurred in this region. The annual mean temperature of this region is 8 °C, with the highest and lowest temperatures occurring in July (24.10 °C) and January (−4.53 °C), respectively. The annual mean precipitation ranges from 600 to 650 mm, mainly focused in July and August, whereas the mean annual evaporation is approximately 1510 mm.

2.2 Tree-ring data

In June 2009, Chinese pine tree-ring samples were collected from three different sites in the Lingkong Mountain area (Fig. 1). The first sampling site (112°5.227′ E, 36°35.588′ N, 1480–1700 m a.s.l.) was in the national nature reservation park of Lingkong Mountain, labeled LKS, where 60 tree-ring cores from 30 living trees were extracted using the increment borer. The second site (112°5.20′ E, 36°46.38′ N, 1450–1650 m a.s.l.) was located to the northwest of LKS, and labeled WJW, 40 tree-ring cores from 20 living trees were collected from this area. At the third site (112°24.62′ E, 36°53.97′ N, 1450 m a.s.l.), eight cores from four trees were collected, this site was named JF. The distance between the three sites was greater than 30 km.

Tree-ring samples were processed according to the standard dendrochronological technique (Cook and Kairiukstis, 1990). All the tree rings in each core were measured to the nearest 0.01 mm. The COFECHA program (Holmes, 1983) was utilized to estimate the quality of crossdating and ring-width measurements. Series with short ages or that were abnormal in comparison with the majority of series were discarded from the chronology construction. Because the COFECHA results showed that strong similarities existed among the ring-width series from different sites, we finally combined all of the samples into one group. Standardization is a basic step in dendrochornology to remove the non-climate trends related to tree age or the effects of stand dynamics by fitting a curve to each raw measurement series and index for each core was calculated by dividing the actual ring width by the corresponding fitted value (Cook and Kairiukstis, 1990). All individual indices were then combined to produce a single chronology

by means of "biweight robust mean". Here, we employed negative exponential curve or straight line with negative slope as fitted curves. Implementation of the standardization was performed using the ARSTAN program (Cook, 1985). A subsample signal strength (SSS) threshold of 0.85 (Wigley et al., 1984) was applied to assess the reliable starting year of the chronology, excluding the low quality of earlier years due to low sample size. The signal strength of the chronology was also evaluated over time using statistics of the calculated running series of average between-tree correlations (RBAR) (Briffa and Jones, 1990) and the running express population signal (EPS) (Wigley et al., 1984) based on a 50 yr window.

2.3 Meteorological data

Two meteorological stations are located near the sampled sites (Fig. 1). The nearest station is Jiexiu (111°55′ E, 37°02′ N, 743.9 m a.s.l.) and the other is Linfen (111°30′ E, 36°04′ N, 450.3 m a.s.l.). Both stations have 55 yr instrumental records spanning from 1954 to 2008 AD. As shown in Fig. 2, monthly precipitation and mean temperature records at the two stations showed similar variation, indicating a regional coherence of climate. Therefore, the monthly precipitation amount and monthly mean temperature records from the two stations were extracted. Palmer drought severity index (PDSI) is a metric that can be used to effectively evaluate moisture condition in an area (Dai et al., 2004) and has been applied in dendroclimatological studies to determine moisture conditions worldwide (Cook et al., 2010; Tei et al., 2013). In the present paper, PDSI data from 1954 to 2005 AD from the nearest point (111.25° E, 36.25° N) were also chosen to compare with the tree-ring index.

2.4 Statistical analysis

Climate–growth relationships were investigated using Pearson correlation analysis between the tree-ring chronology and the meteorological records as well as the PDSI data. A simple linear regression model was adopted to reconstruct the mean PDSI

Reconstruction of the March–August PDSI based on tree rings of Chinese pine

Q. Cai et al.

value from March to August. The fidelity of the reconstruction was verified by comparison with the instrumental PDSI data and checked by the leave-one-out cross-validation method (Michaelsen, 1987). Furthermore, the stability of the regression model was also tested by applying the Bootstrap (Cook and Kairiukstis, 1990) and Jackknife (Efron, 1979) statistical methods, which have been adopted in dendroclimatology (Liu et al., 2013). The temporal and spatial representativeness of the PDSI reconstruction was tested by comparisons with other tree-ring-based moisture indexes from nearby area and spatial correlation analysis between the instrumental and reconstructed March–August PDSI and the PDSI grid dataset according to KNMI Climate Explore (http://climexp.knmi.nl). Multi-taper spectral analysis (MTM) (Mann and Lees, 1996) was conducted to identify the periodicities in the reconstructed series.

3 Results

3.1 Tree-ring chronology

All of the final 88 ring-width measurements from the three different sites were highly correlated ($r = 0.71$), and were successfully combined to develop a regional tree-ring chronology spanning from 1617 to 2008 AD (Fig. 3). The most credible starting year of the chronology was 1703 AD, corresponding to 10 trees based on the SSS > 0.85 criterion. During the reliable period of the chronology, the mean EPS value was greater than 0.94, far higher than the acceptable threshold of 0.85 (Wigley et al., 1984), and RBAR also showed high and stable value (Fig. 3). The signal to noise ratio (SNR) was 36.36, and variance in the first eigenvector (PC1) was 42.52, demonstrating strong signal strength among all trees involved in the chronology.

3.2 Ring growth–climate relationship

Because the tree-ring chronology had similar response to the climatic factors of the two meteorological stations, we only showed the results between the tree-ring index

and climatic factors from the Jiexiu station. As shown in Fig. 4a, the regional tree-ring chronology showed positive correlation with the monthly precipitation amount of previous September (0.48) and current May (0.42) at the 0.01 confidence level. Additionally, significant negative relationships were found with the monthly mean temperature of March (-0.41), May (-0.5) and June (-0.45) at the 0.01 confidence level and with the monthly mean temperature of February (-0.31) and July (-0.28) at the 0.05 confidence level.

Similar to studies in other areas of northern China (Fang et al., 2009; Cai and Liu, 2013), correlations of tree rings with monthly PDSI were much higher than with precipitation or temperature (Fig. 4b). The most significant ($p < 0.01$) correlations was found in May (0.68) and June (0.69) followed by July (0.62) and March (0.6). Although the highest correlation was observed between tree rings and the monthly combination of PDSI from May to June ($r = 0.697$, $p < 0.001$), March–August PDSI ($r = 0.681$, $p < 0.001$) was chosen for the reconstruction considering that both the moisture conditions in spring (March to May) and summer (June to August) are pivotal for agricultural production (Ma et al., 2006; Xiao et al., 2007) and tree growth in northern China (Du et al., 2007; Cai et al., 2008; Koretsune et al., 2009; Cai and Liu, 2013).

3.3 PDSI reconstruction

Using the tree-ring chronology from Lingkong Mountain (RC) as predictor, a simple linear regression model ($PDSI_{38} = 7.517 \times RC - 8.631$) was designed to reconstruct March–August PDSI ($PDSI_{38}$) variation. Figure 5a demonstrates that the reconstructed PDSI simulates the instrumental record very well. The reconstruction could explain 46.4 % of the instrumental record (45.3 % after adjustment for the loss of degrees of freedom) over the calibration period from 1954 to 2005 AD. In case of high correlation caused by trends, the correlation coefficient (r) between the two first difference series of reconstruction and instrumental data was also calculated (Fig. 5b). The r value was 0.66, indicating a high coherence between high frequency variation of the reconstructed and instrumental series.

The results of the leave-one-out test are shown in Table 1. The sign test (S, S1) between the instrumental and estimated PDSI series, and between the first difference series of the two PDSI datasets, are significant at the 99 % confident level. The product means value (t) is 3.07 and the reduction of error (RE) is positive, indicating sufficient similarity exists between the reconstructed and instrumental data. The statistical results of Bootstrap and Jackknife analysis are shown in Table 2. The values of r, R^2 (R^2_{adj}), standard error of estimate, F and P closely resemble the statistics determined for the total dataset. The above tests indicate that the regression model is stable and suitable for further PDSI reconstruction.

We subsequently extended the March–August mean PDSI variation back to 1703 AD (Fig. 6a), the longest series in the eastern part of the CLP to date. The reconstruction exhibited considerable fluctuations on both the annual and decadal scales.

4 Discussions

4.1 Annual, inter-annual and centennial variation of the PDSI

The mean PDSI value of the reconstruction over the entire study period (1703–2008 AD) was −1.45, and the standard deviation (σ) was 2.23. By defining extremely wet years as those having values greater than 0.78 (mean $+1\sigma$) and extremely dry years as values lower than −3.68 (mean $−1\sigma$), the 10 driest yeas were identified as 1810 (−7.50), 1900 (−7.20), 1721 (−7.16), 1916 (−6.52), 2000 (−6.45), 1759 (−6.41), 1747 (−6.38), 1902 (−6.29), 1892 (−6.25) and 1870 (−6.18), and the top 10 wettest years were 1857 (5.51), 1948 (4.86), 1950 (4.58), 1949 (4.18), 1946 (3.92), 1956 (3.16), 1934 (3.15), 1938 (2.86), 1736 (2.85) and 1782 (2.78), respectively.

Persistent drought event usually has more significant impact on agricultural products and social stability than that of single year (Xiao et al., 2011). Overall, seven comparatively dry and six comparatively wet periods were observed based on the 11 yr moving average of the reconstruction (Table 3).

During the past 306 yr, 1867–1932 AD was the longest dry period in the reconstruction (with 10 yr disturbance of normal years from 1880–1890 AD); the mean PDSI value of this duration was −2.62, and the mean value of its early part (1867–1879 AD) was −3.88, indicating that this was the driest period in the reconstruction (Fig. 6a). Historical documents recorded three distinguished consecutive drought events in northern China caused by climate change since the Qing Dynasty during 1719–1723, 1876–1878 and 1927–1930, respectively (Zeng et al., 2009; Hao et al., 2010). Among them, the 1876–1878 and 1927–1930 drought events ranked as two of the most severe natural disasters in Chinese history and have drawn significant attention from scientists due to their devastating consequences on society (Hao et al., 2010; Zhou et al., 2010). These two recent extremely dry events, the 1920s drought in particular, have been captured by many other tree-ring reconstructions in the CLP and other regions of China (Liu et al., 2003a, b, 2005, 2010; Liang et al., 2007; Chen et al., 2011, 2012; Deng et al., 2013; Kang et al., 2013) as well as Mongolia (Pederson et al., 2001). The 1920s drought was also revealed by a weakened signal of the EASM indicated by a dry-wet mode index (Qian et al., 2012). In the present paper, these two drought events were also revealed by very low PDSI values during 1876–1878 (−5.02) and 1928–1931(−3.86) (Fig. 6a). However, the drought in 1719–1723 is seldom mentioned in previous dendroclimatological reports due to the limited length of reconstruction (Fang et al., 2010a, 2013). In this study of Lingkong Mountain, 1721 was identified as the third driest years, and 1719–1726 was identified as one of the dry periods during the past 306 yr (Table 3). The mean PDSI value from 1721 to 1723 was −4.39, which is much lower than the mean PDSI value of this reconstruction. This drought was also recorded by a joint investigation based on drought/flood index and tree-ring records in 1720–1722 at Luya Mountain (Yi et al., 2012), which is approximately 700 km north of studied area. The above analysis demonstrated the ability of this PDSI reconstruction to reproduce the drought history in the Lingkong Mountain area, even northern China.

Moreover, 1934–1957 AD was the longest and wettest period in the reconstruction, with a mean PDSI value of 1.36, corresponding to a strong EASM stage (Liu et al.,

2003b). This wet phenomenon was also captured by tree-ring records from different areas of Inner Mongolia and Korea (Liu et al., 2003b; Liang et al., 2007; Chen et al., 2012) as well as by studies from other regions of northern China (Fig. 7).

The PDSI reconstruction indicates a decreasing trend since 1958 AD, especially after the mid of 1960s, implying a gradually deteriorating moisture condition in the studied area against the background of global warming. The evident dry time appeared during 1993–2008 AD. The drying trend at Lingkong Mountain in recent decades is also accorded with the weakening of East Asian monsoon since the mid of 1960s (Guo et al., 2004; Zeng et al., 2009).

As indicated by the accumulated anomalies (AC) of the PDSI reconstruction (Fig. 6b), which can effectively evaluate long-term trends of dryness and wetness (Tian et al., 2007), the reconstructed March–August PDSI showed clearly centennial variations. The studied area was comparatively wet during the 18th century, with a slight increasing trend of AC from 1703 to 1806. From 1807 to 1932, AC generally indicated a long and sharp decreasing trend, demonstrating a persistent dry time. From 1932 to the end of the 1950s, a sharply increased AC was observed, followed by a comparatively stable stage of AC during the 1960s–1980s, showing a comparatively wet condition; however, after the 1990s, AC decreased sharply, which meant a clearly dry time appeared. Therefore we could say that the 19th century was the driest century of the past three centuries at Lingkong Mountain. Similar conclusions have also been drawn concerning Mongolia (Pederson et al., 2001) and northeastern China (Chen et al., 2011, 2012), as well as the eastern central High Asia (Fang et al., 2010b) based on tree-ring materials.

4.2 Temporal and Spatial representation of the PDSI reconstruction

The dry (wet) durations in our reconstruction not only agree well with the nearby PDSI reconstructions (Figs. 1 and 7) for the Guancen Mountian (Fig. 7b, Sun et al., 2012) and the Taihang Mountain (Fig. 7c, Cai and Liu, 2013), but are also comparable to those from the Ortindag Sand Land, east Inner Mongolia (Fig. 7d, Liang et al., 2007)

and Kongtong Mountains (Fig. 7e, Song and Liu, 2011), which are far to the northeast and the west from the studied sites, respectively. The dry period at 1870s–1880s and the end of the 1920s and the wet period around the 1950s are observed in almost all of the series. Compared with the comparatively longer PDSI reconstruction in the Kongtong Mountians (Fig. 7e), the wet durations during 1727–1741, 1751–1757, 1779–1805 and 1853–1864 AD were approximately synchronous at these two sites, and the dry periods during 1742–1748, 1771–1778, 1807–1818 and the longest dry period during 1867–1932 AD were comparable, although differences existed in the intensity and length of their durations. Moreover, our PDSI reconstruction was also comparable to a nearby tree-ring-based March–July runoff reconstruction for the upper Fenhe River basin (Sun et al., 2013) and tree-ring based precipitation reconstruction of Helan Mountain in north-central China (Liu et al., 2005).

The climate in northern China is known to be strongly affected by the EASM system. Abnormal behaviors of the EASM often result in floods or droughts in the monsoon region. Zhou et al. (2009) reconstructed a June–August Asian–Pacific Oscillation index (I_{APO}) to investigate the long-term variation of the EASM. The calculated correlation coefficient (r) between our reconstructed PDSI and the I_{APO} was 0.29 (1703–1985, $p < 0.001$), and r was 0.44 ($p < 0.001$) after the two series were smoothed using an 11 yr moving average (Fig. 8). All of the series in Fig. 7 correspond to special regions influenced by the EASM, and thus, the isochronous variation of the moisture indicators at different sites is intuitively shown.

The instrumental March–August PDSI of the Lingkong Mountains exhibited significant and positive correlation with the March–August PDSI grid dataset over a sizable region around the studied site in the CLP, and also showed significant positive correlations with that of middle-east Inner Mongolia and east Mongolia during 1954–2005 AD (Fig. 9a). A similar correlation pattern was observed between the reconstructed March–August PDSI and the PDSI grid dataset (Fig. 9b), which tentatively indicated that our PDSI reconstruction successfully simulated the instrumental PDSI values and

can be used to indicate the moisture conditions for a broad region surrounding the Lingkong Mountain in the CLP over the past 306 yr.

4.3 Possible linkage with ENSO and solar activity

Variation of the EASM is induced by large-scale thermal difference between the land and sea, and it is closely related to tropical and subtropical sea-surface temperature associated ENSO, which has proven to be a crucial factor influencing climate in northern China (Wang et al., 2000, 2008). In this work, the MTM results revealed 2.0–2.1, 2.5, 2.6, 2.7, 3.0–3.1, 3.5, 3.9 and 7.6–7.8 yr cycles (Fig. 10). These cycles are very similar to those of ENSO (Diaz and Markgraf, 2000), showing the possible influence of ENSO on the moisture variability in the studied area. These 2–7 yr cycles have also been widely reported in previous tree-ring studies in China (Liang et al., 2007; Fang et al., 2009; Chen et al., 2011; Liu et al., 2011; Cai and Liu, 2013). The 37.9 yr cycle was very similar to the 38 yr cycle in the 2485 yr temperature reconstructions in the northeastern Tibetan Plateau (Liu et al., 2011), to the 35–38 yr cycle in a tree-ring-based streamflow reconstruction for the upper Yellow River (Gou et al., 2010) and to the 34.1 yr cycle in a tree-ring network-based spatial drought reconstruction for central high Asia (Fang et al., 2010b). Considering the limited length of our reconstruction (306 yr), the 102 yr cycle ($p < 0.01$) may not be reliable. However, century-scale variations were important cycles of solar activity, which complexly influence the Earth's climate (Liu et al., 2011). A similar centennial spectrum peak was identified in the Heng Mountain area of northern China (Cai and Liu, 2013) and the northeastern Tibetan Plateau (Liu et al., 2011). Both the 37.9 and 102 yr cycles resemble the 35 yr Bruckner (Raspopov et al., 2004) and Gleissberg cycles of solar activity (Sonett et al., 1990; Braun et al., 2005), respectively, which supports the influence of solar activity on moisture variations in the Lingkong Mountain area.

5   Conclusions

Using a moisture-limited regional tree-ring chronology developed from Lingkong Mountain in the southeast CLP, we reconstructed the March–August mean PDSI variations from 1703 to 2008 with an explained variance of 46.4 %. The reconstructed PDSI simulated the instrumental PDSI reasonably well and exhibited considerable fluctuations on both the annual and decadal scales. It revealed seven comparatively dry and six comparatively wet periods over the past 306 yr. 1867–1932 and 1934–1957 AD were the longest dry and wet period, respectively. The three extreme drought events during 1719–1723, 1876–1878 and 1927–1930 in northern China since the Qing Dynasty were successfully captured in our reconstruction, demonstrating its ability to reproduce the drought history in the Lingkong Mountain area. The warm and dry phases of Lingkong Mountain were in accordance with changes in the EASM strength, suggesting the influence of EASM and related factors (e.g. ENSO) on the moisture conditions in the studied area. The PDSI reconstruction was temporally and regionally representative by comparing with other tree-ring based moisture reconstructions around the studied site in northern China and spatial correlation analysis, although differences existed in the intensity and length of the warm/dry durations in different areas. This manuscript not only contributes a new dataset for this area, stepping forward to a much denser and wider drought-sensitive tree-ring network, but also provides new insights into long-term regional moisture variations and offers a reference for future regional drought forecasts. In the future, more efforts are still needed to collect more old trees from CLP to extend the moisture reconstruction far back in time.

References

Braun, H., Christl, M., Rahmstorf, S., Ganopolski, A., Mangini, A., Kubatzki, C., Roth, K., and Kromer, B.: Possible solar origin of the 1470 yr glacial climate cycle demonstrated in a coupled model, Nature, 438, 208–211, 2005.

Briffa, K. R. and Jones, P. D.: Basic chronology statistics and assessment, in: Methods of Dendrochronology, edited by: Cook, E. R. and Kairiukstis, L. A., Kluwer Academic Publishers, Dordrecht, 137–152, 1990.

Büntgen, U., Tegel, W., Nicolussi, K., McCormick, M., Frank, D., Trouet, V., Kaplan, J. O., Herzig, F., Heussner, K.-U., Wanner, H., Luterbacher, J., and Esper, J.: 2500 yr of European climate variability and human susceptibility, Science, 331, 578–582, 2011.

Cai, Q. F. and Liu, Y.: Climatic response of Chinese pine and PDSI variability in the middle Taihang Mountains, north China since 1873, Trees, 27, 419–427, 2013.

Cai, Q. F., Liu, Y., Song, H. M., and Sun, J. Y.: Tree-ring-based reconstruction of the April to September mean temperature since 1826 AD for north-central Shaanxi Province, China, Sci. China Ser. D, 51, 1099–1106, 2008.

Cai, Q. F., Liu, Y., and Tian, H.: A dendroclimatic reconstruction of May–June mean temperature variation in north China since 1767 AD, Quatern. Int., 283, 3–10, 2013.

Chen, F., Yuan, Y. J., and Wei, W. S.: Climatic response of Picea crassifolia tree-ring parameters and precipitation reconstruction in the western Qilian Mountains, China, J. Arid Environ., 75, 1121–1128, 2011.

Chen, Z. J., He, X. Y., Cook, E. R., He, H. S., Chen, W., Sun, Y., and Cui, M. X.: Detecting dryness and wetness signals from tree-rings in Shenyang, Northeast China, Palaeogeogr. Palaeocl., 302, 301–310, 2011.

Chen, Z. J., Zhang, X. L., Cui, M. X., He, X. Y., Ding, W. H., and Peng, J. J.: Tree-ring based precipitation reconstruction for the forest–steppe ecotone in northern Inner Mongolia, China and its linkages to the Pacific Ocean variability, Global Planet. Change, 86–87, 45–56, 2012.

Cook, E. R.: A time-series analysis approach to tree-ring standardization, Dissertation for the Doctoral Degree, The University of Arizona, Tucson, 1985.

Cook, E. R. and Kairiukstis, L. A.: Methods of dendrochronology: applications in the environmental sciences, Kluwer Academic Publishers, Dordrecht, 394 pp., 1990.

Title Page

Abstract | Introduction

Conclusions | References

Tables | Figures

|◄ | ►|

◄ | ►

Back | Close

Full Screen / Esc

Printer-friendly Version

Interactive Discussion

Cook, E. R., Anchukaitis, K. J., Buckley, B. M., D'Arrigo, R. D., Jacoby, G. C., and Wright, W. E.: Asian monsoon failure and megadrought during the last millennium, Science, 328, 486–489, 2010.

Dai, A. G., Trenberth, K. E., and Qian, T.: A global dataset of Palmer drought severity index for 1870–2002: relationship with soil moisture and effects of surface warming, J. Hydrometeorol., 5, 1117–1130, 2004.

Deng, Y., Gou, X. H., Gao, L. L., Zhao, Z. Q., Cao, Z. Y., and Yang, M. X.: Aridity changes in the eastern Qilian Mountains since AD 1856 reconstructed from tree-rings, Quatern. Int., 283, 78–84, 2013.

Diaz, H. F. and Markgraf, V.: El Niño and the Southern Oscillation: Multiscale Variability and Global and Regional Impacts, Cambridge University Press, 496 pp., 2000.

Du, S., Norikazu, Y., Fukuju, Y., Kyoichi, O., Wang, S. Q., and Hou, Q. C.: The effect of climate on radial growth of *Quercus Liaotungensis* forest trees in Loess Plateau, China, Dendrochronologia, 25, 29–36, 2007.

Efron, B.: Bootstrap methods: another look at the jackknife, Ann. Stat., 7, 1–26, 1979.

Esper, J., Frank, D., Büntgen, U., Verstege, A., Luterbacher, J., and Xoplaki, E.: Long-term drought severity variations in Morocco, Geophys. Res. Lett., 34, L17702, doi:10.1029/2007GL030844, 2007.

Fang, K. Y., Gou, X. H., Chen, F. H., Yang, M. X., Li, J. B., He, M. S., Zhang, Y., Tian, Q. H., and Peng, J. F.: Drought variations in the eastern part of northwest China over the past two centuries: evidence from tree rings, Clim. Res., 38, 129–135, 2009.

Fang, K. Y., Gou, X. H., Chen, F. H., D'Arrigo, R., and Li, J. B.: Tree-ring based drought reconstruction for the Guiqing Mountain (China): linkages to the Indian and Pacific Oceans, Int. J. Climatol., 30, 1137–1145, 2010a.

Fang, K. Y., Davi, N., Gou, X. H., Chen, F. H., Cook, E., Li, J. B., and D'Arrigo, R.: Spatial drought reconstructions for central High Asia based on tree rings, Clim. Dynam., 35, 941–951, 2010b.

Fang, K. Y., Gou, X. H., Chen, F. H., Liu, C. Z., Davi, N., Li, J. B., Zhao, Z. Q., and Li, Y. J.: Tree-ring based reconstruction of drought variability (1615–2009) in the Kongtong Mountain area, northern China, Global. Planet. Change, 80–81, 190–197, 2012.

Fang, K. Y., Frank, D., Gou, X. H., Liu, C. Z., Zhou, F. F., Li, J. B., and Li, Y. J.: Precipitation over the past four centuries in the Dieshan Mountains as inferred from tree rings: an introduction to an HHT-based method, Global. Planet. Change, 107, 109–118, 2013.

Reconstruction of the March–August PDSI based on tree rings of Chinese pine

Q. Cai et al.

Gao, P., Mu, X.-M., Li, R., and Wang, F.: Analyses of relationship between Loess Plateau erosion and sunspots based on wavelet transform, Hydrol. Earth Syst. Sci. Discuss., 8, 277–303, doi:10.5194/hessd-8-277-2011, 2011.

Gao, S. Y., Lu, R. J., Qiang, M. R., Hasi, E. D., Zhang, D. S., Chen, Y., and Xia, H.: Reconstruction of precipitation in the last 140 yr from tree ring at south margin of the Tengger Desert, China, Chin. Sci. Bull., 50, 2487–2492, 2005.

Gou, X. H., Deng, Y., Chen, F. H., Yang, M. X., Fang, K. Y., Gao, L. L., Yang, T., and Zhang, F.: Tree ring based streamflow reconstruction for the Upper Yellow River over the past 1234 yr, Chin. Sci. Bull., 55, 4179–4186, 2010.

Guo, Q. Y., Cai, J. N., Shao, X. M., and Sha, W. Y.: Studies on the variations of East-Asian summer monsoon during AD 1873 ∼ 2000, Chin. J. Atmos. Sci., 28, 206–215, 2004.

Hao, Z. X., Zheng, J. Y., Wu, G. F., Zhang, X. Z., and Ge, Q. S.: 1876–1878 severe drought in North China: facts, impacts and climatic background, Chin. Sci. Bull., 55, 3001–3007, 2010.

Holmes, R. L.: Computer-assisted quality control in tree-ring dating and measurement, Tree-Ring Bull., 43, 69–75, 1983.

Kang, S. Y., Yang, B., Qin, C., Wang, J. L., Shi, F., and Liu, J. J.: Extreme drought events in the years 1877–1878, and 1928, in the southeast Qilian Mountains and the air-sea coupling system, Quatern. Int., 283, 85–92, 2013.

Koretsune, S., Fukuda, K., Chang, Z. Y., Shi, F. C., and Ishida, A.: Effective rainfall seasons for interannual variation in δ^{13}C and tree-ring width in early and late wood of Chinese pine and black locust on the Loess Plateau, China, J. Forest Res., 14, 88–94, 2009.

Liang, E. Y., Liu, X. H., Yuan, Y. J., Qin, N. S., Fang, X. Q., Huang, L., Zhu, H. F., Wang, L. L., and Shao, X. M.: The 1920s drought recorded by tree rings and historical documents in the semi-arid and arid areas of northern China, Climatic Change, 79, 403–432, 2006.

Liang, E. Y., Shao, X. M., Liu, H. Y., and Eckstein, D.: Tree-ring based PDSI reconstruction since AD 1842 in the Ortindag Sand Land, east Inner Mongolia, Chin. Sci. Bull., 52, 2715–2721, 2007.

Linderholm, H. W., Björklund, J. A., Seftigen, K., Gunnarson, B. E., Grudd, H., Jeong, J.-H., Drobyshev, I., and Liu, Y.: Dendroclimatology in Fennoscandia – from past accomplishments to future potential, Clim. Past, 6, 93–114, doi:10.5194/cp-6-93-2010, 2010.

Linderholm, H. W., Liu, Y., Leavitt, S. W., and Liang, E. Y.: Dendrochronology in Asia, Quatern. Int., 283, 1–2, 2013.

Liu, Y., Cai, Q. F. Park, W.-K., An, Z. S., and Ma, L. M.: Tree-ring precipitation records from Baiyinaobao, Inner Mongolia since A. D. 1838, Chin. Sci. Bull., 48, 1140–1145, 2003a.

Liu, Y., Park, W.-K., Cai, Q. F., Seo, J.-W., and Jung, H.-S.: Monsoonal precipitation variation in the East Asia since A. D. 1840: tree-ring evidences from China and Korea, Sci. China Ser. D, 46, 1031–1039, 2003b.

Liu, Y., Cai, Q. F., Shi, J. F., Hughes, M. K., Kutzbach, J. E., Liu, Z. Y., Ni, F. B., and An, Z. S.: Seasonal precipitation in the south-central Helan Mountain region, China, reconstructed from tree-ring width for the past 224 yr, Can. J. Forest. Res., 35, 2403–2412, 2005.

Liu, Y., Tian, H., Song, H. M., and Liang, J. M.: Tree-ring precipitation reconstruction in the Chifeng-Weichang region, China, and East Asian summer monsoon variation since A. D. 1777, J. Geophys. Res., 115, D06103, doi:10.1029/2009JD012330, 2010.

Liu, Y., Cai, Q. F., Song, H. M., An, Z. S., and Linderholm, H. W.: Amplitudes, rates, periodicities and causes of temperature variations in the past 2485 yr and future trends over the central-eastern Tibetan Plateau, Chin. Sci. Bull., 56, 2986–2994, 2011.

Liu, Y., Sun, B., Song, H. M., Lei, Y., and Wang, C. Y.: Tree-ring-based precipitation reconstruction for Mt. Xinglong, China, since AD 1679, Quatern. Int., 283, 46–54, 2013.

Ma, J. J., Gao, X. Q., and Qu, Y. L.: The character of precipitation and its relation to climate change over north China in spring and summer, Clim. Environ. Res., 11, 321–329, 2006.

Ma, Z. G. and Fu, C. B.: Some evidences of drying trend over northern China from 1951 to 2004, Chin. Sci. Bull., 51, 2913–2925, 2006.

Mann, M. E. and Lees, J. M.: Robust estimation of background noise and signal detection in climatic time series, Climatic Change, 33, 409–445, 1996.

Michaelsen, J.: Cross-validation in statistical climate forecast models, J. Climate Appl. Meteorol., 26, 1589–1600, 1987.

Ohyama, M., Yonenobu, H., Choi, J.-N., Park, W.-K., Hanzawa, M., and Suzuki, M.: Reconstruction of northeast Asia spring temperature 1784–1990, Clim. Past, 9, 261–266, doi:10.5194/cp-9-261-2013, 2013.

Pederson, N., Jacoby, G. C., D'Arrigo, R. D., Cook, E. R., Buckley, B. M., Dugarjav, C., and Mijiddorj, R.: Hydrometeorological reconstructions for northeastern Mongolia derived from tree rings: AD 1651–1995, J. Climate, 14, 872–881, 2001.

Qian, W. H., Lin, X., and Zhu, Y. F.: Global and China temperature changes associated with the inter-decadal variations of East Asian summer monsoon advances, Chin. Sci. Bull., 30, 3923–3930, 2012.

Raspopov, O. M., Dergachevb, V. A., and Kolström, T.: Periodicity of climate conditions and solar variability derived from dendrochronological and other palaeo-climatic data in high latitudes, Palaeogeogr. Palaeocl., 209, 127–139, 2004.

Sonett, C. P., Finney, S. A., and Berger, A.: The spectrum of radiocarbon, Phil. T. Roy. Soc. Lond. A, 330, 413–426, 1990.

Song, H. M. and Liu, Y.: PDSI variations at Kongtong Mountain, China, inferred from a 283 yr *Pinus tabulaeformis* ring width chronology, J. Geophys. Res., 116, D22111, doi:10.1029/2011JD016220, 2011.

Sun, J. Y., Liu, Y., Sun, B., and Wang, R. Y.: Tree-ring based PDSI reconstruction since 1853 AD in the source of the Fenhe River Basin, Shanxi Province, China, Sci. China Ser. D, 55, 1847–1854, 2012.

Sun, J. Y., Liu, Y., Wang, Y. C., Bao, G., and Sun, B.: Tree-ring based runoff reconstruction of the upper Fenhe River basin, North China, since 1799 AD, Quatern. Int., 283, 117–124, 2013.

Tei, S., Sugimoto, A., Yonenobu, H., Hoshino, Y., and Maximov, T. C.: Reconstruction of summer Palmer Drought Severity Index from δ^{13}C of larch tree rings in East Siberia, Quatern. Int., 290–291, 275–281, 2013.

Tian, Q. H., Gou, X. H., Zhang, Y., Peng, J. F., Wang, J. S., and Chen, T.: Tree-ring based drought reconstruction (A. D. 1855–2001) for the Qilian Mountains, Northwestern China, Tree-Ring Res., 63, 27–36, 2007.

Wang, B., Wu, R. G., and Fu, X. H.: Pacific-East Asian teleconnection: how does ENSO affect East Asian climate?, J. Climate, 13, 1517–1536, 2000.

Wang, B., Yang, J., Zhou, T. J., and Wang, B. L.: Interdecadal changes in the major modes of Asian-Australian monsoon variability: strengthening relationship with ENSO since the late 1970s, J. Climate, 21, 1771–1789, 2008.

Wang, Y.: The preliminary study on the natural disaster in north Shaanxi during 1923–1931, Meteorol. Disaster Reduc. Res., 29, 34–38, 2006.

Wei, J., Zhang, Q. Y., and Tao, S. Y.: Physical causes of the 1999 and 2000 summer sever drought in north China, Chin. J. Atmos. Sci., 28, 125–137, 2004.

Wigley, T. M. L., Briffa, K. R., and Jones, P. D.: On the average value of correlated time series, with applications in dendroclimatology and hydrometeorology, J. Clim. Appl. Meteorol., 23, 201–213, 1984.

Title Page

Abstract | Introduction

Conclusions | References

Tables | Figures

◄ | ►

◄ | ►

Back | Close

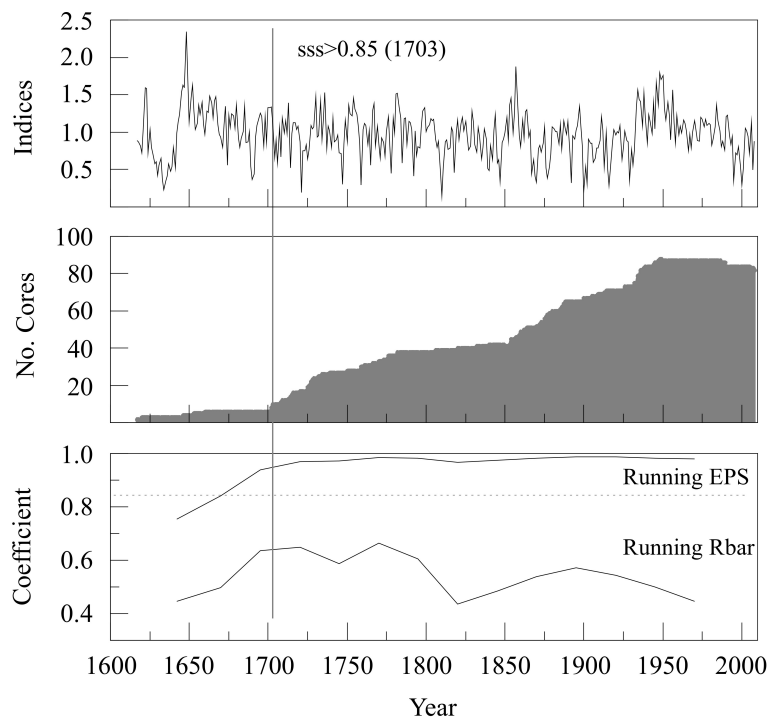Full Screen / Esc

Printer-friendly Version

Interactive Discussion

Xiao, G. J., Zhang, Q., and Xiong, Y. C.: Integrating rainwater harvesting with supplemental irrigation into rain-fed spring wheat farming, Soil Till. Res., 93, 429–437, 2007.

Xiao, L. B., Ye, Y., and Wei, B. Y.: Revolts frequency during 1644–1911 in north China plain and its relationship with climate, Adv. Clim. Change Res., 2, 218–224, 2011.

Xu, J. H.: Sun, climate, famine and folk nation transfer, Sci. China Ser. D, 28, 366–384, 1998.

Yang, B., Bräuning, A., Liu, J. J., Davis, M. E., and Shao, Y. J.: Temperature changes on the Tibetan Plateau during the past 600 yr inferred from ice cores and tree rings, Global. Planet. Change, 69, 71–78, 2009.

Yao, Y. B., Wang, Y. R., Li, Y. H., and Zhang, X. Y.: Climate warming and drying and its environmental effects in the Loess Plateau, Resour. Science, 27, 146–152, 2005.

Yi, L., Yu, H. J., Ge, J. Y., Lai, Z. P., Xi, X. Y., Qom, L., and Peng, S. Z.: Reconstructions of annual summer precipitation and temperature in north-central China since 1470 AD based on drought/flood index and tree-ring records, Climatic Change, 110, 469–498, 2012.

Zeng, G., Ni, D. H., Li, Z. X., and Li, C. H.: Advances in the research of inter-decadal variation of East Asian summer Monsoon, Meteor. Disaster Reduction Res., 32, 1–7, 2009.

Zeng, Z. Z., Fang, X. Q., Ye, Y., and Zhang, X. Z.: Comparison of disaster situation and causes of three extreme droughts in China over the Past 300 Years, J. Catastro., 24, 116–122, 2009.

Zhang, D. D., Lee, H., Wang, C., Li, B., Pei, Q., Zhang, J., and An, Y.: The causality analysis of climate change and large-scale human crisis, P. Natl. Acad. Sci. USA, 108, 17296–17301, 2011.

Zhang, Q. B., Chen, G. D., Yao, T. D., Kang, X. C., and Huang, J. G.: A 2326 yr tree-ring record of climate variability on the northeastern Qinghai-Tibetan Plateau, Geophys. Res. Lett., 30, 1739, doi:10.1029/2003GL017425, 2003.

Zhang, Z. B., Tian, H. D., Cazelles, B., Kausrud, K. L., Bräuning, A., Guo, F., and Stenseth, N. C.: Periodic climate cooling enhanced natural disasters and wars in China during AD 10–1900, P. Roy. Soc. B, 277, 3745–3753, 2010.

Zhou, Q. G., Qu, X. W., and Cheng, Y.: The natural disasters in Northern China during late Qing Dynasty, J. Soc. Sci. Hunan Normal Univ., 2, 122–126, 2010.

Zhou, X. J., Zhao, P., and Liu, G.: Asian-Pacific Oscillation index and variation of East Asian summer monsoon over the past millennium, Chin. Sci. Bull., 54, 3768–3771, 2009.

Zhu, H. F., Fang, X. Q., Shao, X. M., and Yin, Z. Y.: Tree ring-based February–April temperature reconstruction for Changbai Mountain in Northeast China and its implication for East Asian winter monsoon, Clim. Past, 5, 661–666, doi:10.5194/cp-5-661-2009, 2009.

Title Page

Abstract | Introduction

Conclusions | References

Tables | Figures

|◀ | ▶|

◀ | ▶

Back | Close

Full Screen / Esc

Printer-friendly Version

Interactive Discussion

Table 1. Results of the leave-one-out test for the period of 1954–2005 AD.

r	R^2	S	S1	t	RE
0.681	0.464	39+/13−[*]	38+/13−[*]	3.07	0.439

[*] means 99 % confident level

Table 2. Statistics of the regression model.

	Calibration (1954–2005 AD)	Verification (1954–2005 AD)	
		Jackknife Mean (range)	Bootstrap (80 iterations) Mean (range)
r	0.681	0.68 (0.63–0.71)	0.68 (0.47–0.85)
R^2	0.464	0.46 (0.40–0.51)	0.47 (0.22–0.73)
R^2_{adj}	0.453	0.45 (0.38–0.50)	0.46 (0.20–0.72)
Standard error of estimate	1.939	1.94 (1.82–1.96)	1.89 (1.53–2.27)
F	43.26	42.47 (32.18–51.06)	48.30 (13.94–132.75)
P	0.0001	0.0001 (0.00–0.00)	0.0001 (0.00–0.00)

Table 3. Persistent dry and wet periods during 1703–2008 AD.

Dry periods		Wet periods	
Time span	Mean PDSI value	Time span	Mean PDSI value
1719–1726	−3.11	1727–1741	−0.39
1742–1748	−2.94	1751–1757	0.93
1771–1778	−2.44	1779–1787	0.28
1807–1818	−3.21	1797–1805	0.03
1832–1848	−2.78	1853–1864	0.57
1867–1932	−2.62	1934–1957	1.36
1993–2008	−3.03		
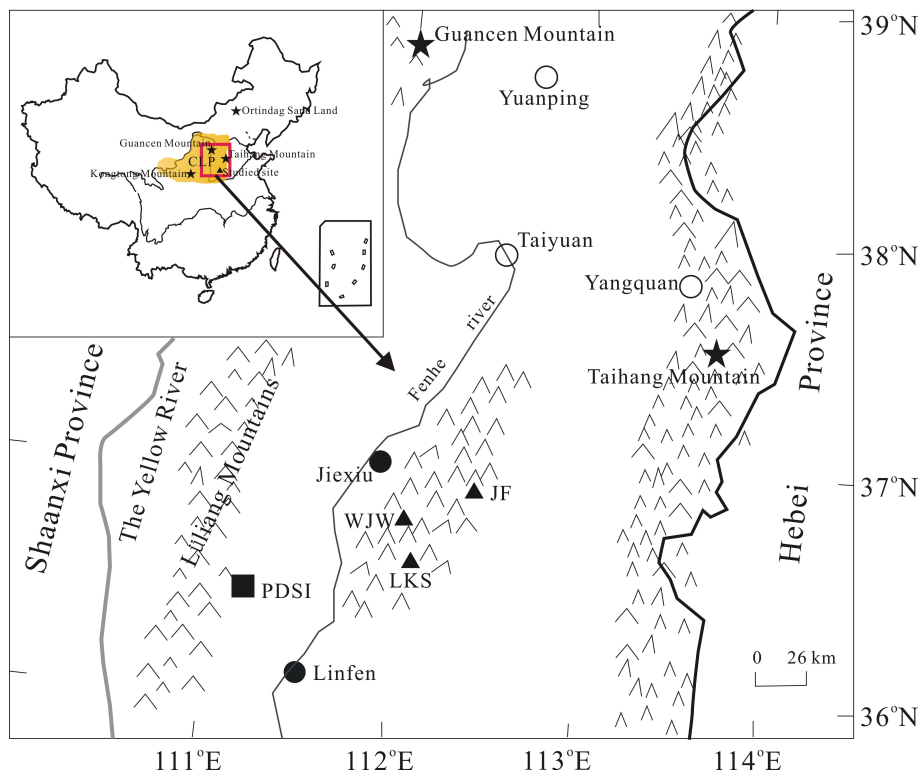
Fig. 1. Location of the sampling sites (▲), meteorological stations (•), PDSI (■) and the compared locations (⋆). The area highlighted in yellow indicates the general location of the Chinese Loess Plateau (CLP).

Fig. 2. Monthly precipitation and monthly mean temperature distribution of the two meteorological stations from 1954–2008 AD.

Fig. 3. (a) The regional tree-ring chronology of Lingkong Mountain, **(b)** number of cores and **(c)** EPS and RBAR statistics.

Title Page

Abstract | Introduction

Conclusions | References

Tables | Figures

|◄ | ►|

◄ | ►

Back | Close

Full Screen / Esc

Printer-friendly Version

Interactive Discussion

Full Screen / Esc

Printer-friendly Version

Interactive Discussion
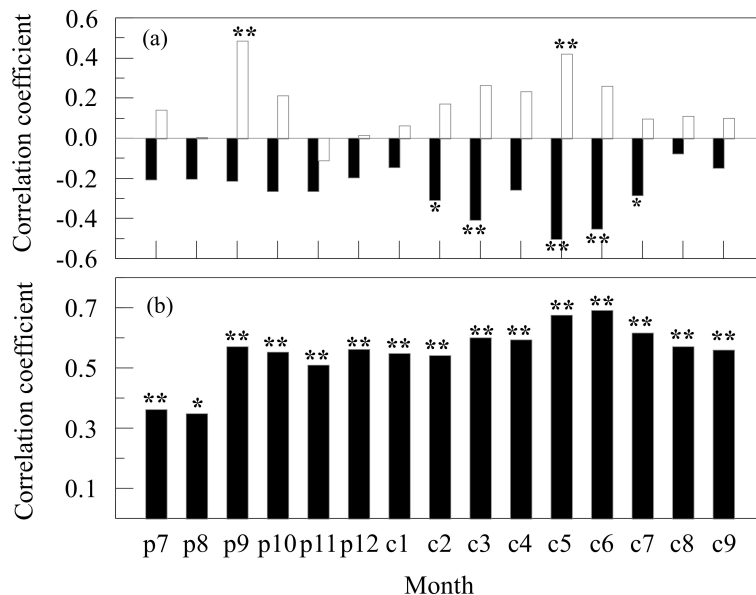
Fig. 4. Correlations of the ring-width indices with **(a)** the monthly mean temperature (black bars) and monthly precipitation (white bars) records obtained from the Jiexiu station during 1954–2008 AD and **(b)** PDSI data during the interval of 1954–2005 AD. * indicates correlations exceeding the 0.05 confidence level; ** indicates correlations exceeding the 0.01 confidence level; p: previous year; c: current year.
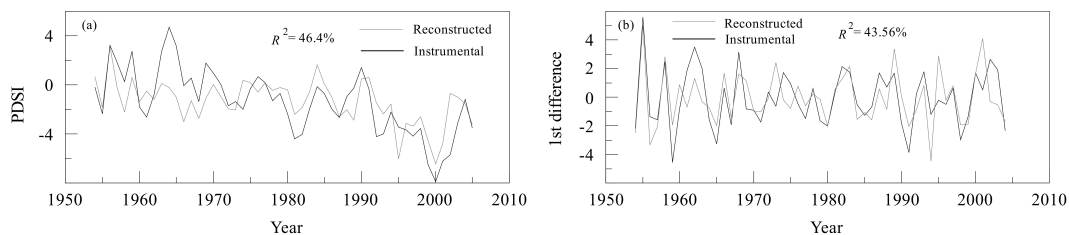
Fig. 5. Comparisons **(a)** between reconstructed and instrumental PDSI, and **(b)** between the first differences of reconstructed and instrumental PDSI over their common period of 1954–2005 AD.

Discussion Paper | Discussion Paper | Discussion Paper | Discussion Paper

CPD

9, 6311–6344, 2013

Reconstruction of the March–August PDSI based on tree rings of Chinese pine

Q. Cai et al.

Title Page

Abstract Introduction

Conclusions References

Tables Figures

|◄ ►|

◄ ►

Back Close

Full Screen / Esc

Printer-friendly Version

Interactive Discussion
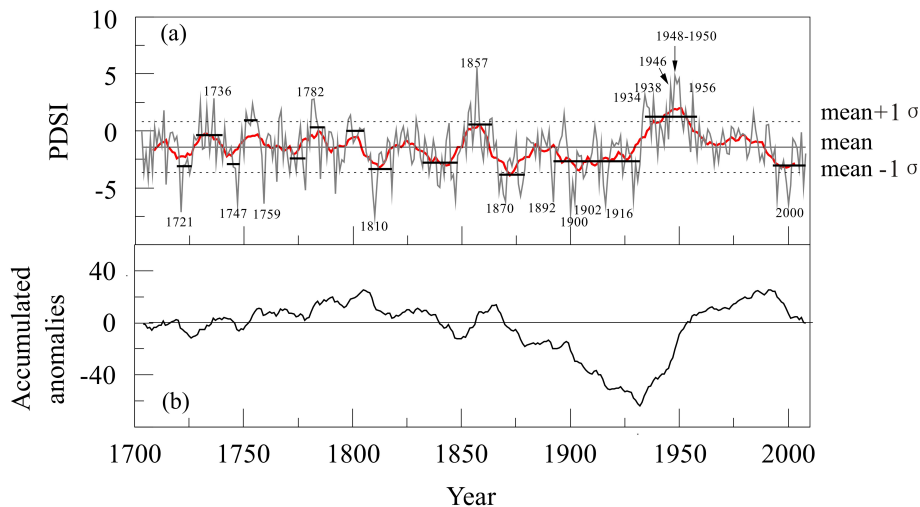
Fig. 6. (a) March–August PDSI reconstruction from 1703 to 2008 AD. The thick red line is the 11 yr moving average, the long horizontal line is the mean PDSI value of 1703–2008 AD, and the short horizontal lines are the mean PDSI values for different dry/wet periods; **(b)** accumulated anomalies (AC) of the PDSI reconstruction.
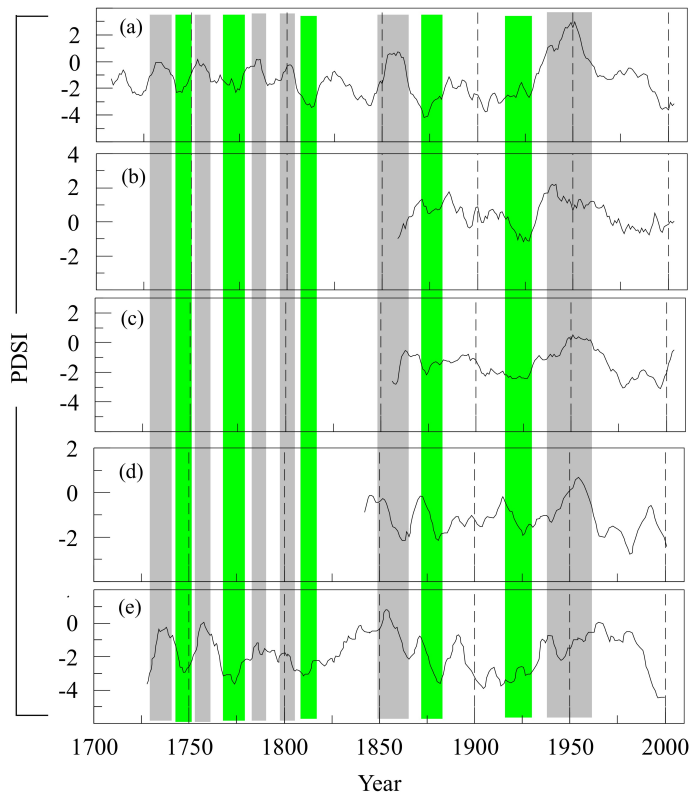
Fig. 7. Comparisons of the March–August mean PDSI reconstruction **(a)** with the April–July PDSI reconstruction of the Guancen Mountain (Sun et al., 2012) **(b)**, the May–June mean PDSI of the Taihang Mountain (Cai and Liu, 2013a) **(c)**, the May–July PDSI reconstruction in the Ortindag Sand Land, east Inner Mongolia (Liang et al., 2007) **(d)**, and **(e)** the May–July mean PDSI reconstruction for the Kongtong Mountain, Gansu Province (Song and Liu, 2011). The lines are the 11 yr moving average. Green and grey bars show the dry and wet periods, respectively.

Discussion Paper | Discussion Paper | Discussion Paper | Discussion Paper |

CPD

9, 6311–6344, 2013

Reconstruction of the March–August PDSI based on tree rings of Chinese pine

Q. Cai et al.

Title Page

Abstract | Introduction

Conclusions | References

Tables | Figures

|◄ | ►|

◄ | ►

Back | Close

Full Screen / Esc

Printer-friendly Version

Interactive Discussion
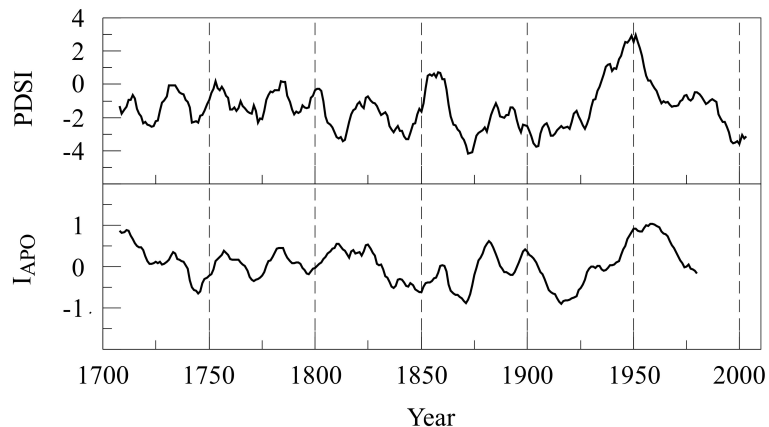
Fig. 8. Comparison between the 11 yr moving average of this reconstruction (top panel) and the summer I_{APO} (bottom panel) (Zhou et al., 2009).
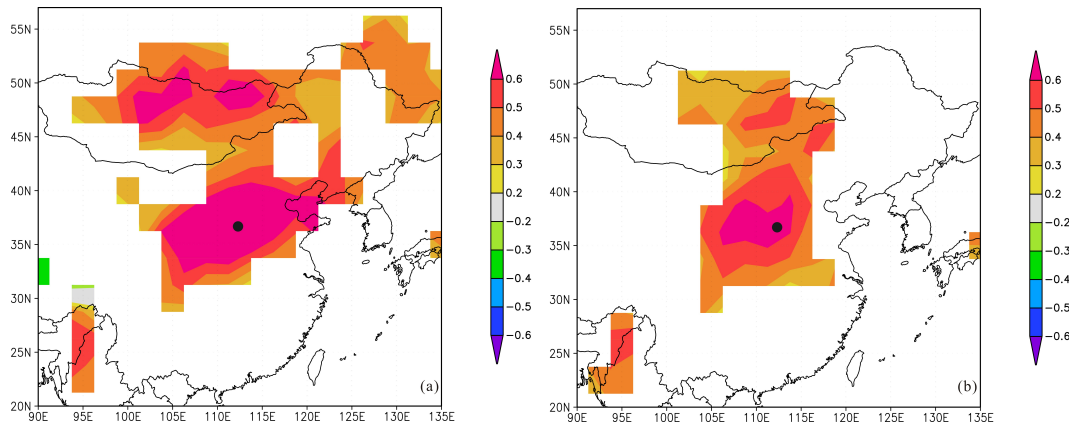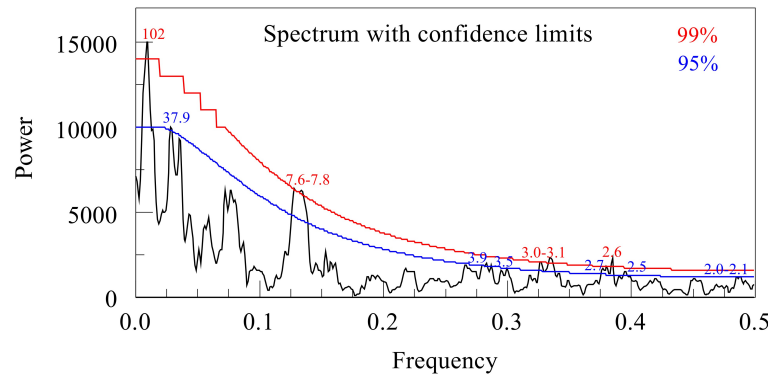
Fig. 9. Spatial correlations between the instrumental **(a)** and reconstructed **(b)** PDSI of March–August and the concurrent grid data set of the PDSI over their overlapping periods (1954–2005) (http://climexp.knmi.nl). The black dot indicates our sampling site.

Full Screen / Esc

Printer-friendly Version

Interactive Discussion

Fig. 10. The multi-taper spectrum analysis of the reconstructed PDSI. The blue line and red line show the 95 and 99 % confidence limits, respectively.